Nitrous oxide production and consumption by marine ammonia-oxidizing archaea under oxygen depletion

Elisa Hernández-Magaña* and Beate Kraft*

Nordcee, Department of Biology, Faculty of Sciences, University of Southern Denmark, Odense, Denmark

Ammonia-oxidizing archaea (AOA) are key players in the nitrogen cycle and among the most abundant microorganisms in the ocean, thriving even in oxygen-depleted ecosystems. AOA produce the greenhouse gas nitrous oxide (N_2O) as a byproduct of ammonia oxidation. Additionally, the recent discovery of a nitric oxide dismutation pathway in the AOA isolate *Nitrosopumilus maritimus* points toward other N_2O production and consumption pathways in AOA. AOA that perform NO dismutation when exposed to oxygen depletion, produce oxygen and dinitrogen as final products. Based on the transient accumulation of N_2O coupled with oxygen accumulation, N_2O has been proposed as an intermediate in this novel archaeal pathway. In this study, we spiked N_2O to oxygen-depleted incubations with pure cultures of two marine AOA isolates that were performing NO dismutation. By using combinations of N compounds with different isotopic signatures ($^{15}NO_2^-$ pool $+^{44}N_2O$ spike and $^{14}NO_2^-$ pool $+^{46}N_2O$ spike), we evaluated the N_2O spike effects on the production of oxygen and the isotopic signature of N_2 and N_2O. The experiments confirmed that N_2O is an intermediate in NO dismutation by AOA, distinguishing it from similar pathways in other microbial clades. Furthermore, we showed that AOA rapidly reduce high concentrations of spiked N_2O to N_2. These findings advance our understanding of microbial N_2O production and consumption in oxygen-depleted settings and highlight AOA as potentially important key players in N_2O turnover.

KEYWORDS

oxygen depletion, anoxia, NO dismutation, ammonia-oxidizing archaea, nitrous oxide, nitrous oxide reduction

Introduction

Environments with low oxygen concentrations are major sources of the greenhouse gas nitrous oxide (N_2O). Nearly half of the net yearly production of N_2O in the open ocean occurs in hypoxic and oxygen-depleted waters (Codispoti, 2010). N_2O has a warming potential approximately 300 times higher than CO_2 and contributes to stratospheric ozone destruction (IPCC, 2014). In order to understand the dynamics of N_2O emissions from oxygen-depleted environments, it is crucial to disentangle the contributions of different microbial pathways of N_2O production and consumption.

Ammonia-oxidizing archaea (AOA) are key players in the nitrogen cycle, performing the first step of nitrification. They are among the most abundant microorganisms in the ocean, and in some cases, they can represent up to 40% of the total picoplankton in the water column

(Karner et al., 2001). Oceanic ammonia oxidation is almost entirely performed by AOA, and they have been suggested to be an important source of N_2O in the ocean (Santoro et al., 2011; Löscher et al., 2012). Here, N_2O is mainly formed as a byproduct of ammonia oxidation in a process named hybrid formation. In this process, hydroxylamine from NH_4^+ reacts with NO, which is produced from NO_2^- (Stieglmeier et al., 2014; Kozlowski et al., 2016; Prosser et al., 2020; Wu et al., 2020; Stein et al., 2021).

Until the recent discovery of the NO-dismutation pathway in AOA upon oxygen depletion, AOA were assumed to be inactive when oxygen was absent. In this NO-dismutation pathway, AOA reduces NO_2^-, which is the product of aerobic ammonia oxidation, to NO. Then, NO is dismutated to O_2 and N_2O, which is reduced to N_2 (Kraft et al., 2022). The dismutation step is thermodynamically favorable ($2NO \rightarrow N_2O + 0.5O_2$, $\Delta G0' = -165kJ/mol\ O_2$), and AOA can use the produced oxygen to fuel ammonia oxidation (Kraft et al., 2022). N_2O is proposed to be an intermediate based on the transient accumulation of $^{15,15}N$-labeled N_2O from ^{15}N-nitrite in parallel to oxygen production (Kraft et al., 2022; Hernández-Magaña et al., 2023). NO dismutation has been observed previously in the methane-oxidizing bacterium *Ca. Methylomirabilis oxyfera*, which also produces O_2 and N_2 as final products of the pathway (Ettwig et al., 2010). However, there is no evidence of N_2O production or reduction associated with this process. A further difference is that in the case of *Ca. M. oxyfera*, the oxygen produced is immediately utilized to oxidize methane and other microbial processes (Ettwig et al., 2010). In the case of AOA, the oxygen produced during NO dismutation is used for ammonia oxidation and respiration, but the coupling between production and consumption is not that tight, and oxygen accumulates (Kraft et al., 2022).

AOA are highly abundant in environments with low or undetectable oxygen concentrations, such as anoxic basins such as the Black Sea (Sollai et al., 2019) or oceanic oxygen minimum zones (OMZs) (Francis et al., 2005; Lam et al., 2007; Beman et al., 2008; Peng et al., 2015; Bristow et al., 2016). The discovery of NO dismutation in AOA provides a potential explanation for their presence in these environments, suggesting that AOA may contribute to N_2O cycling if N_2O indeed is an intermediate in NO dismutation.

To date, N_2O production from nitrite in anoxic environments has been solely attributed to denitrification. Denitrification, the stepwise reduction of nitrate to dinitrogen ($NO_3^- \rightarrow NO_2^- \rightarrow NO \rightarrow N_2O \rightarrow N_2$), can be performed by a phylogenetically diverse group of organisms, including bacteria, archaea, and eukaryotes (Thomson et al., 2012). Some denitrifiers possess only some of the enzymes and can only carry out incomplete denitrification; organisms that cannot reduce N_2O to N_2 lead to the accumulation of N_2O (Babbin et al., 2015), while some microorganisms that only reduce N_2O to N_2 become net sinks of N_2O in the system (Jones et al., 2013). Biogeochemical rate measurements based on ^{15}N-stable isotope labeling would not be able to distinguish between denitrification and NO dismutation as sources for N_2O and N_2 production because, in both processes, the two N atoms originate from nitrite.

To test the role of N_2O as an intermediate in the NO dismutation pathway by AOA, we carried out incubations under oxygen depletion with pure cultures of the AOA strains, *N. maritimus* and *Nitrosopumilus piranensis*. The oxygen-depleted incubations were combined with the use of ^{15}N-stable isotope-labeled compounds to track the origin and fate of the nitrogen gases N_2O and N_2 during NO

dismutation. The N_2 and N_2O accumulation patterns from different experiments support the role of N_2O as an intermediate in the formation of N_2 upon oxygen depletion. Furthermore, solid evidence for the N_2O reduction to N_2 by two marine AOA isolates is presented.

Materials and methods

Growth conditions

Axenic 5 L batch pre-cultures of the AOA strains *N. maritimus* SCM1 and *N. piranensis* D3C (JCM 32271, DSM 106147, and NCIMB 15115) were grown at 28°C in the dark in synthetic Crenarchaeota medium (SCM) HEPES-buffered (pH 7.8), as described by Könneke et al. (2005) and Martens-Habbena et al. (2009), modified with a 6 mM final concentration of sodium bicarbonate (Kraft et al., 2022).

Oxygen-depleted incubations

The oxygen-depleted incubations were prepared by sparging the aerobically grown batch culture with argon gas (99.99%) for 45 min to reduce the oxygen concentration in the culture. The culture was sterilely transferred into 330-ml custom-made glass bottles designed to avoid oxygen intrusion with a glass capillary and a port for inserting a microsensor (Tiano et al., 2014) through a glass tube connection, using the overpressure generated in the argon-sparged culture bottle. All bottles were filled without headspace and closed with glass stoppers. The bottles were continuously stirred with glass-coated stirring bars (VWR, United Kingdom) at 300 rpm. The bottles were incubated in a water bath at 28°C in the dark. Control incubations with the custom-made bottles and killed controls with $HgCl_2$ have been previously reported in Kraft et al. (2022), showing no oxygen intrusion from the atmosphere.

Oxygen was monitored constantly during the incubations with trace fluorescence oxygen sensors, also referred to as optodes, with a detection limit of 0.5 nM (Lehner et al., 2015). The optodes were previously glued to the glass bottles. NO was monitored with microsensors (Unisense, Denmark), inserted into the sensor ports of the bottles, which were previously sterilized with 70% ethanol, and rinsed with autoclaved ASTM1a water. NO was observed to cause a small and predictable interference with the optodes (up to 17%). Therefore, the oxygen concentration measurements were corrected for NO interference, as in Kraft et al. (2022). All bottles, stirring bars, tube connections, and materials used for the incubation were previously autoclaved.

N_2O as an intermediate in dinitrogen production via NO dismutation

Two sets of experiments with ^{15}N-stable isotope compounds were used for the identification of the intermediates in dinitrogen and oxygen production via NO dismutation.

For the first experimental setup, batch cultures of *N. maritimus* and *N. piranensis* were grown aerobically with ^{15}N-labeled ammonium ($^{15}NH_4^+$) until it was completely oxidized to $^{15}NO_2^-$, and thus cultures

contained a pool of 1 mM of $^{15}NO_2^-$ (late exponential phase). Prior to the incubation, more than 500 μM of $^{14}NH_4^+$ was added to the culture to ensure the survival (ammonia oxidation) of the cultures during the experiment and to capture traces of $^{15}NH_4^+$ that could have remained in a large pool of $^{14}NH_4^+$. The incubations under oxygen depletion were set up, as described in the section "oxygen-depleted incubations." The sets of replicates (at least 3 bottles of 330 mL each per incubation) were spiked with 1.2 μM of unlabeled N_2O ($^{44}N_2O$) after 30 h in the case of *N. maritimus* and with 3 μM after 6 h and 1.2 μM after 30 h in the case of *N. piranensis*. Three incubation replicates were kept without the addition of N_2O as a control. A killed control was performed by adding mercury chloride to the incubation.

In the second set of experiments, an aerobically grown batch culture of *N. piranensis* was maintained with $^{14}NH_4^+$ until it was completely oxidized to $^{14}NO_2^-$. Then, the batch culture contained a pool of approximately 1 mM of $^{14}NO_2^-$ (the late exponential phase). Prior to the incubation, more than 500 μM of $^{14}NH_4^+$ was added to the culture to ensure the survival (ammonia oxidation) of the cultures during the experiment. The oxygen-depleted incubation was started, as described in the section "oxygen-depleted incubations." One set of replicates (at least three bottles of 330 mL each) was spiked with 40 nM of ^{15}N-labeled N_2O ($^{46}N_2O$) at 8 h and with 90 nM at 42 h. Three incubation replicates were kept without the addition of $^{46}N_2O$ as a control.

Sample collection and analysis

Samples were collected with gas-tight syringes (Hamilton, United States) that were connected to stainless steel needles (Ochs, Germany) through the capillaries of the incubation bottles. When collecting the samples, the volume collected was simultaneously replaced with deoxygenated sterile culture media to avoid headspace formation in the incubation bottle. The samples were collected in 3-ml gas-tight exetainers, headspace-free, and preserved with 50 μL of saturated $HgCl_2$ solution. The isotopic signature of N_2 and N_2O was analyzed by coupled gas chromatography–isotope ratio mass spectrometry (GC-IRMS) on a Thermo Delta V Plus isotope ratio mass spectrometer (Dalsgaard et al., 2012). Total N_2O concentrations were analyzed using a gas chromatograph (GC-TRACE1300, Thermo Scientific) equipped with an electron capture detector. Concentrations were plotted as the average of at least three replicates, with error bars representing the standard deviation. Rates were calculated from the change in concentration over time, with $r^2 > 0.9$.

Results

Reduction of N_2O to N_2 by *N. maritimus* and *N. piranensis* under oxygen depletion

The AOA strains *N. maritimus* and *N. piranensis* were previously observed to conduct NO dismutation upon oxygen depletion (Kraft et al., 2022; Hernández-Magaña et al., 2023), in which they produced oxygen and ultimately N_2 from NO_2^-. Transient accumulation of N_2O in both strains was reported in the cited publications, suggesting that AOA can produce N_2O under oxygen depletion and further reduce it to N_2. To assess the role of N_2O as an intermediate in NO dismutation

by AOA and, therefore, the AOA's potential to reduce N_2O, we performed incubations under oxygen depletion with pure cultures of *N. maritimus* and *N. piranensis*. The first set of incubations was started with a pool of $^{15}NO_2^-$ and spiked with 1.2–1.5 μM of unlabeled nitrous oxide ($^{44}N_2O$) at 30 h for both AOA strains and additionally with 3 μM of $^{44}N_2O$ at 6 h only for *N. piranensis*.

A striking decrease in the total N_2O concentration was observed after the spike in all the incubations. N_2O consumption was especially fast within the first 3 h after the spike (Figure 1). For example, *N. piranensis* consumed on average 497 nM/h in the first 3 h after the 6-h spike and 198 nM/h after the 30-h spike. Overall, strikingly fast N_2O consumption after the spikes was consistently observed in all the incubations. After this first fast decrease in N_2O, N_2O consumption slowed down. Then, *N. maritimus* had the highest consumption rate of 48 nM/h, followed by the incubation of N. piranensis after the spike at 6 h, which had a rate of 41 nM/h. Finally, the same strain after the spike at 30 h consumed all spiked N_2O in approximately 30 h at a rate of 28 nM/h. The accumulation of $^{46}N_2O$ from $^{15}NO_2^-$ started within the first hours of the oxygen-depleted incubations, followed by a linear production of $^{30}N_2$ (Figure 2, controls). In *N. maritimus* incubations, the production of $^{30}N_2$ increased at approximately 20 h, while in *N. piranensis* N_2 production was linear from the beginning of the oxygen-depleted incubation. Another subtle difference between the strains was the transient accumulation of N_2O, which was maintained throughout the whole incubation period for *N. maritimus*. For *N. piranensis*, the N_2O accumulation started quickly after oxygen depletion, reaching its maximum within the first 20 h and decreasing almost totally after 40 h of oxygen depletion. Despite these differences in accumulation patterns between strains, there is consistency in the transient accumulation of $^{46}N_2O$ and in the formation of $^{46}N_2O$ only from $^{15}NO_2^-$ via NO, which is consistent with previous observations (Kraft et al., 2022; Hernández-Magaña et al., 2023).

If N_2O is a free intermediate in the NO-dismutation pathway (a product of the NO-dismutation step), which is reduced to N_2 and not a byproduct, an increase in the pool of $^{44}N_2O$ over $^{46}N_2O$ ($^{44}N_2O$ spike) would lead to an increase in $^{28}N_2$ production instead of $^{30}N_2$ production compared to the control incubations, in which only $^{46}N_2O$ is available. Thus, the reduction of N_2O from a pool enriched with $^{44}N_2O$ would be observed as a slowing of $^{30}N_2$ accumulation. For the incubation with *N. maritimus* in which $^{44}N_2O$ was spiked at 30 h (Figure 1A), $^{30}N_2$ accumulation stopped until the spiked $^{44}N_2O$ was consumed (55 h) and then $^{30}N_2$ accumulation started again (Figure 2A), demonstrating the direct reduction of N_2O to N_2 and the role of N_2O as an intermediate in the NO-dismutation pathway. For the incubations with *N. piranensis*, a similar pattern in $^{30}N_2$ production was observed after the spike of $^{44}N_2O$ at 6 h of the incubation (Figure 2C). In the case of the spiked incubations of *N. piranensis* at 30 h, the effect of the $^{44}N_2O$ spike on the $^{30}N_2$ production was more difficult to notice in the averaged trend (Figure 2B) and easier to distinguish in the trends of the individual replicates (Supplementary Figure S1A). The replicate with the fastest total N_2O consumption (Supplementary Figure S1B) was the only replicate with no visible effect on the $^{30}N_2$ production after the 30-h spike (Supplementary Figure S1A), suggesting that the N_2O pool was consumed too fast to capture the N_2O produced from nitrite. Additionally, no production of $^{30}N_2$ or $^{46}N_2O$ or consumption of N_2O after a spike of $^{44}N_2O$ was detected in the killed control with *N. maritimus* (Supplementary Figure S2), indicating that the consumption of N_2O was performed by active cells of AOA.
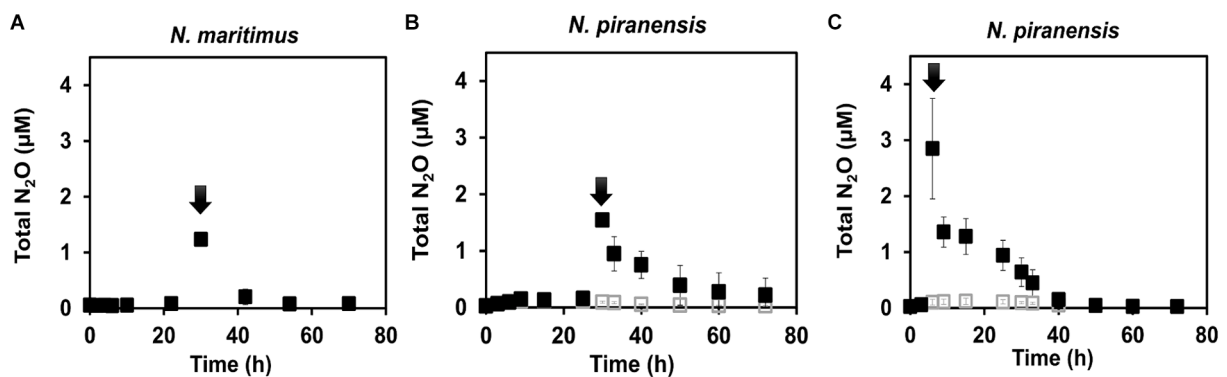
FIGURE 1
N_2O consumption in oxygen-depleted incubations of AOA cultures receiving a spike of N_2O (black arrows). **(A)** *N. maritimus* spiked with 1.2 μM of $^{44}N_2O$ at 30 h of incubation. **(B)** *N. piranensis* spiked with 1.5 μM of $^{44}N_2O$ at 30 h of incubation. **(C)** *N. piranensis* spiked with 3 μM of $^{44}N_2O$ at 6 h. Filled squares show the spiked incubations, while open squares are control replicates (without spike). Symbols represent averages of triplicates, and error bars represent the standard deviation. Some error bars are smaller than the symbols.
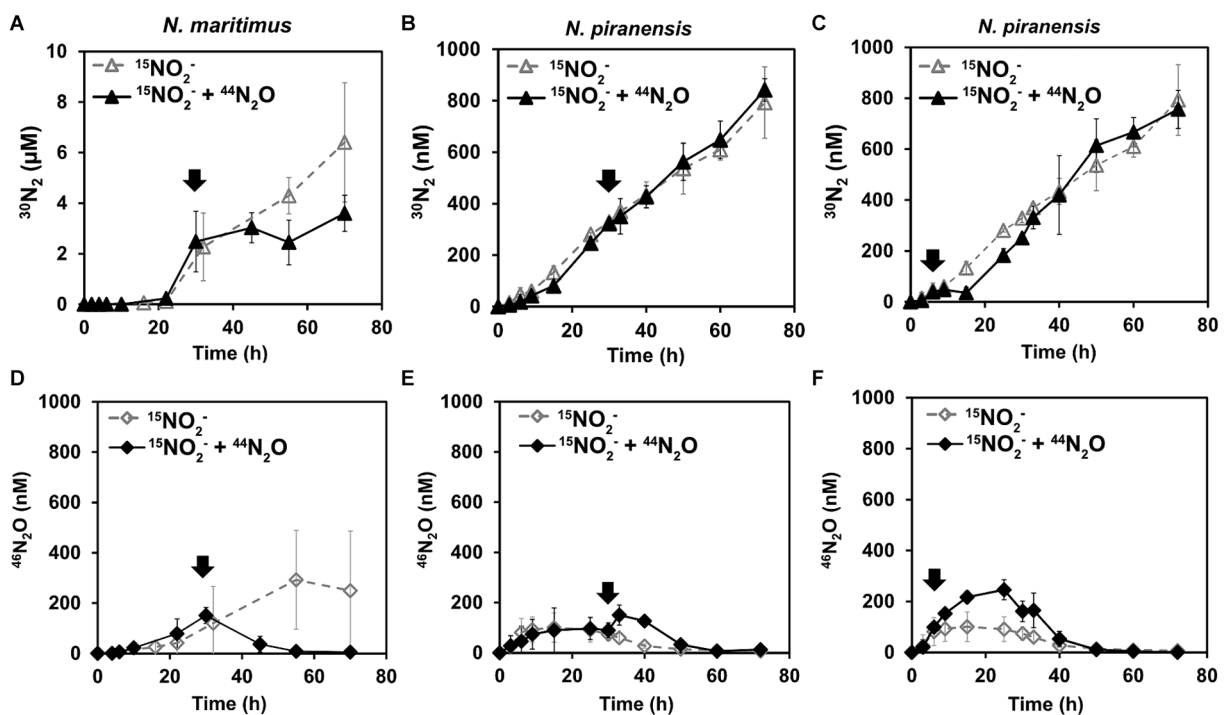

FIGURE 2
Effect of $^{44}N_2O$ spikes on $^{30}N_2$ and $^{46}N_2O$ accumulation by AOA under oxygen depletion. All incubations started with a pool of $^{15}NO_2^-$, and $^{44}N_2O$ was spiked (marked by arrows). The top panels show the accumulation trends of $^{30}N_2$, while the bottom panels show the parallel $^{46}N_2O$ accumulation for the same set of incubations: **(A,D)** from *N. maritimus* with $^{44}N_2O$ spiked at 30 h **(B,E)** from *N. piranensis* with $^{44}N_2O$ spiked at 30 h, and **(C,F)** from *N. piranensis* with $^{44}N_2O$ spiked at 6 h. Open symbols represent control incubations (only $^{15}NO_2^-$ pool), while black symbols show the spiked treatment. The average values of at least three replicates are presented; error bars represent the standard deviation. Some error bars are smaller than the symbols and are therefore not visible.

Complementary incubations to the previous ones were performed to further explore the ability of AOA to reduce N_2O to dinitrogen. *N. piranensis* was selected based on the observations in previous incubations that pointed toward a faster N_2O turnover during NO dismutation. For these incubations, the concentration of spiked N_2O was reduced so that the total N_2O concentration remained in the range in which *N. piranensis* was previously observed to accumulate, to better simulate the conditions under which the reduction of N_2O to

N_2 naturally takes place. To track the outcome of the small spikes of N_2O in this set of incubations, the ^{15}N-labeled compound was N_2O and not nitrite. Oxygen-depleted incubations were performed with a batch culture with a pool of $^{14}NO_2^-$. After 8 h, 40 nM of $^{46}N_2O$ was spiked into the incubation bottles. The added $^{46}N_2O$ was completely consumed approximately 24 h after the spike at a rate of approximately 1.5 nM/h (Figure 3A). After 42 h of incubation, a second addition of $^{46}N_2O$ was made, this time aiming for a final concentration of

approximately 90 nM. The $^{46}N_2O$ added was rapidly consumed again the second time at a rate of approximately 3.5 nM/h.

$^{30}N_2$ production was only observed in the replicates spiked with $^{46}N_2O$ (Figure 3B) and was within the expected range. After the second spike, up to 106 ± 2 nM of $^{30}N_2$ was produced by the end of the incubation (Figure 3B), indicating a complete conversion of the spiked $^{46}N_2O$ to N_2. The measured $^{46}N_2O$ spike was 38 ± 9 nM in the first spike and 89 ± 4 nM in the second spike. Thus, the incubation received a total of 127 ± 9 nM $^{46}N_2O$. Every time a sample was collected, the volume was replaced with anoxic sterile medium (see Materials and Methods), leading to a dilution of the added $^{46}N_2O$ and the produced $^{30}N_2$. Taking this into account, the expected concentration of $^{15\text{-}15}N$ compounds at the end of the incubation was 106 nM (see Supplementary material), consistent with the $^{30}N_2$ accumulated by the end of the incubation. To summarize, the spiked $^{46}N_2O$ was completely reduced to and recovered as $^{30}N_2$.

In the controls that did not receive any ^{15}N-labeled compounds, accumulation of neither $^{30}N_2$ nor $^{46}N_2O$ was observed. In these incubations, the accumulation of unlabeled N_2O started in all replicates at the beginning of the incubation and continued until the spike. After the $^{46}N_2O$ spike, the total N_2O concentration ($^{44}N_2O + {}^{46}N_2O$) was slightly higher in the spiked replicates compared to the controls. Overall, the total N_2O concentration remained within the natural range in which *N. piranensis* would normally accumulate (Supplementary Figure S3). Taken together, the results of both sets of incubations present solid evidence for N_2O turnover by AOA under oxygen depletion and support its role as an intermediate in the NO-dismutation metabolic pathway.

Oxygen accumulation dynamics in *N. maritimus* and *N. piranensis*

In order to resolve trends in oxygen consumption and accumulation, oxygen concentrations were measured during all incubations with sensors that can resolve oxygen concentrations in the nanomolar range (Lehner et al., 2015). In all incubations, the oxygen was respired within the first few minutes after the transfer to the incubation bottles. For *N. maritimus*, shortly after the oxygen was depleted, oxygen started to accumulate, coupled with NO accumulation (Figure 4A). This pattern of oxygen accumulation has been reported previously by Kraft et al. (2022) for *N. maritimus* and for other AOA species, including *N. piranensis*, by Hernández-Magaña et al. (2023). When samples were collected, despite the precautions taken (see methodology), the sampling was always accompanied by a small intrusion of oxygen, hereafter referred to as oxygen pulses. Immediately after the oxygen pulses caused by the sampling, oxygen was respired until depletion and oxygen accumulation started again, which was consistently within the nanomolar range and coupled with the transient N_2O accumulation and N_2 production described in the previous section.

In addition to the overall oxygen trends described, there was some variability between strains and among incubations. In the incubations with *N. maritimus*, sometimes there was a decrease in oxygen accumulation toward the end of the incubations (Figure 4A and Supplementary Figure S4A), as also observed by Kraft et al. (2022). NO accumulated coupled with oxygen accumulation, especially within the first 20 h of the incubation, reached its highest concentration during this time. Like oxygen, NO accumulation decreased toward the end of the incubation (Supplementary Figure S4B). Oxygen was still consumed following oxygen pulses, indicating the culture's activity. The cessation of oxygen accumulation should not necessarily be interpreted as a lack of oxygen production, but most likely as a more efficient use of it, as in the case of the methane oxidizer *Ca. Methylomirabilis oxyfera*, which internally consumes all the oxygen produced via NO dismutation (Ettwig et al., 2010).

In the case of *N. piranensis*, variability in oxygen accumulation trends between different culture batches was observed. In some incubations, oxygen accumulated after its consumption (Figure 4B), but in other cases, no oxygen accumulation was observed (Figures 4C,D). However, NO, N_2O, and N_2 accumulation from NO_2 were still observed during these incubations. A possible explanation for the lack of oxygen accumulation while the production of N_2 continued is that NO dismutation continued and the produced oxygen was used more efficiently, as mentioned above. A possible contamination of the culture, which could also lead to the consumption of oxygen produced during incubation, was excluded by fluorescence microscopy.
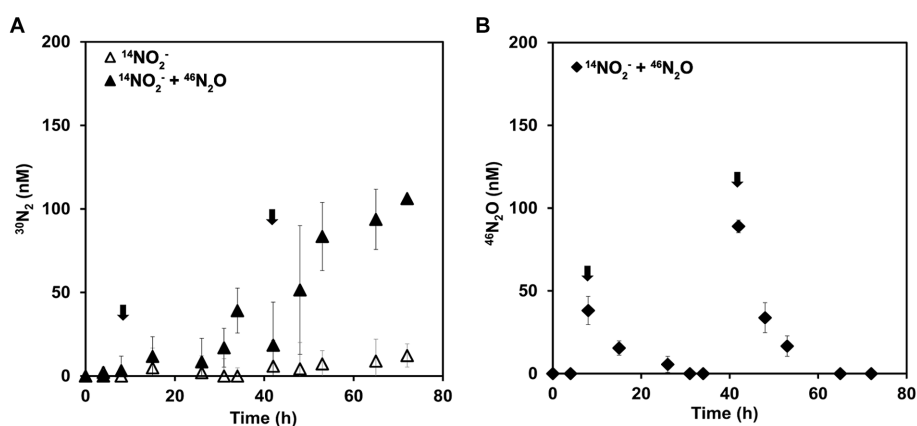
FIGURE 3
$^{46}N_2O$ turnover in oxygen-depleted incubation of *N. piranensis* under oxygen depletion. Incubations started with a pool of $^{14}NO_2^-$ and $^{46}N_2O$ was spiked at 6 h and 42 h (black arrows). **(A)** $^{30}N_2$ production. Black triangles represent incubations into which $^{46}N_2O$ was spiked; open triangles indicate controls without spikes. **(B)** $^{46}N_2O$ concentration measured in the incubation. Black diamonds represent the incubations in which $^{46}N_2O$ was added. $^{46}N_2O$ was undetectable in the control replicates; thus, symbols are not presented. The average of at least three replicates is presented; error bars represent the standard deviation. Some error bars are smaller than the symbols and therefore not visible.

FIGURE 4
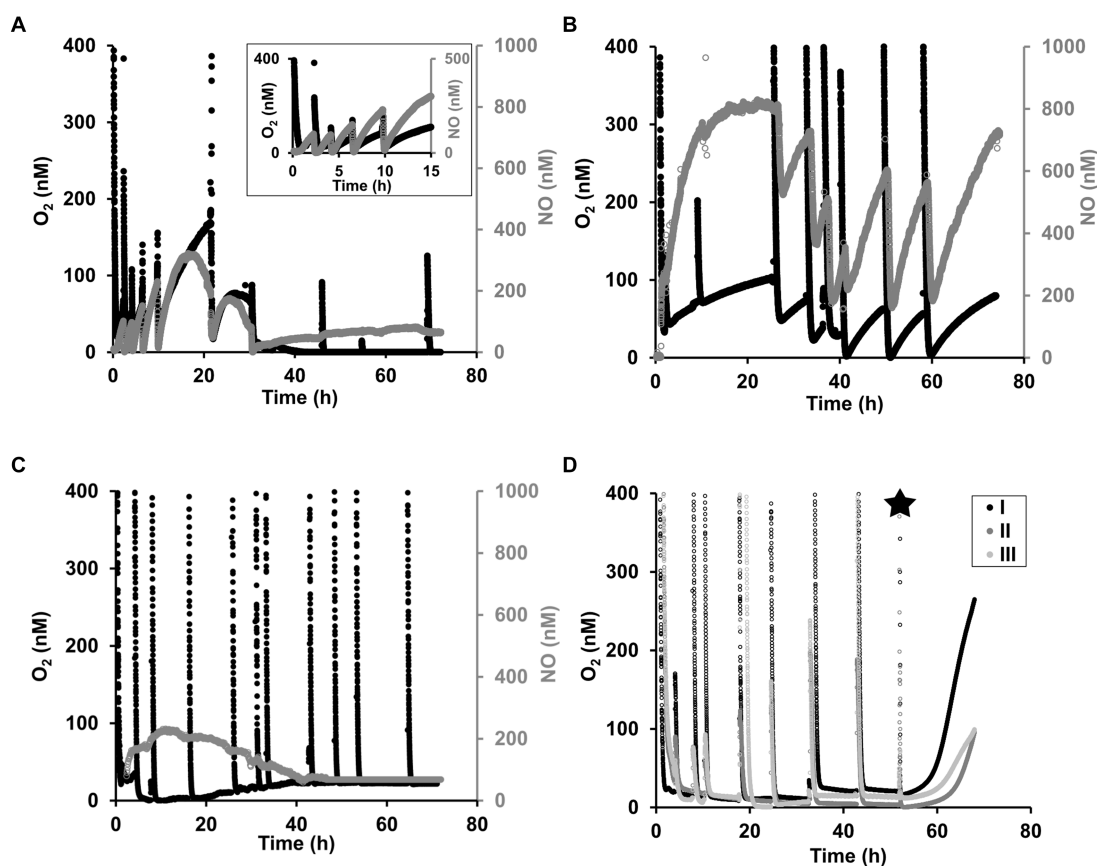Oxygen dynamics in the nanomolar range in oxygen-depleted incubations for *N. maritimus* and *N. piranensis*. **(A)** Oxygen accumulation (black) and NO accumulation (gray) by *N. maritimus* under oxygen depletion. This example of oxygen accumulation corresponds to the incubations of *N. maritimus* started with a $^{15}NO_2^-$ pool and a spike of $^{44}N_2O$ at 30 h (Figures 1, 2). One out of three reproducible replicates is shown, and the other replicates are shown in Supplementary Figure S4, S5. **(B)** *N. piranensis* accumulated oxygen (black) and NO (gray) in different batch incubations. One out of three reproducible replicates is shown here, and the other replicates are shown in Supplementary Figure S6. This incubation was not used for the N_2O spike experiments reported in the present study, but the starting conditions were the same (NO_2^- pool and oxygen depletion). In some batches of *N. piranensis*, oxygen was quickly respired but not accumulated after depletion. **(C)** Shows an example of this. Transient N_2O accumulation and N_2 production were observed in parallel (Figures 1, 2, *N. piranensis*). The example here corresponds to the control incubations with $^{14}NO_2^-$ without spike (The other replicates are shown in Supplementary Figure S7A). The spike of $^{46}N_2O$ at 8 h and at 42 h (Supplementary Figure S6B) did not show differences in oxygen trends. **(D)** After KCN addition (black star), oxygen builds up in incubations with *N. piranensis*. The example here corresponds to the control of the incubations with $^{15}NO_2^-$ without spike. No differences in oxygen trends between control and N_2O spiked replicates were observed (Supplementary Figure S8). Transient N_2O accumulation and N_2 production were observed in parallel (*N. piranensis*, Figures 1, 2).

To test whether *N. piranensis* consumed oxygen more efficiently and thus prevented its accumulation, in some sets of incubations, 0.5 mM of potassium cyanide was added to inhibit oxygen respiration by heme–copper oxygen reductases (Wilson et al., 1994). Indeed, after cyanide addition, oxygen accumulated rapidly (Figure 4D and Supplementary Figure S8A), confirming that oxygen was still being produced but was consumed directly, preventing the accumulation of detectable oxygen concentrations.

Discussion

Marine ammonia-oxidizing archaea reduce N₂O to dinitrogen under oxygen depletion

Oxygen and dinitrogen production through NO dismutation has been observed so far in several different marine and terrestrial AOA isolates, including *N. maritimus* (Kraft et al., 2022) and *N. piranensis* (Hernández-Magaña et al., 2023), which we selected to study the pathway in more detail. In the proposed NO-dismutation pathway, the product of ammonia oxidation, NO_2^-, is reduced to NO, which is dismutated. The proposed products of the dismutation step are N_2O and O_2. N_2O is then further reduced to N_2, making it an intermediate in the NO-dismutation pathway. Transient N_2O accumulation was observed from the beginning of the incubations, followed by N_2 accumulation when *N. maritimus* and *N. piranensis* were exposed to oxygen depletion (this study, Kraft et al., 2022; Hernández-Magaña et al., 2023). The production of N_2O and oxygen from NO dismutation by AOA is a substantial difference from the other known NO-dismutation metabolism by *Ca. M. oxyfera*. This bacterium directly produces N_2 and oxygen via NO dismutation without N_2O as an intermediate (Ettwig et al., 2010). By using a combination of oxygen-depleted incubations with different ^{15}N-labeled compounds and N_2O spikes with different isotopic signatures, we confirmed that

N$_2$O is the direct intermediate of NO dismutation by AOA. Furthermore, the investigated AOA isolates not only turn over N$_2$O from NO dismutation but rapidly reduce externally supplied N$_2$O to N$_2$.

Although the production and accumulation of N$_2$O by AOA had been previously reported (Santoro et al., 2011; Löscher et al., 2012), they had been mainly attributed to hybrid formation from ammonia oxidation products and nitrite in oxic incubations (Stieglmeier et al., 2014; Kozlowski et al., 2016; Hink et al., 2017). The N$_2$O produced in the mentioned studies showed a hybrid isotopic signature, suggesting that one of the N atoms originated from hydroxylamine and one from NO$_2$. A recent study by Wan et al. (2023), using dual-isotope labeling, assessed multiple N$_2$O formation mechanisms by *N. maritimus* and suggested ammonia as the main source of N atoms in N$_2$O under oxic conditions. The same study also found that the production of N$_2$O from nitrite only occurred by hybrid formation when ammonia and oxygen were present. Under the oxygen concentrations used by Wan et al. (2023), the ^{46}N$_2$O formation from ^{15}NO$_2^-$ was negligible, and the authors suggested that the production of N$_2$O by NO dismutation in AOA is restricted to anoxia. In our experiments, the isotopic signature of the N$_2$O accumulated by *N. maritimus* and *N. piranensis* upon oxygen depletion (^{46}N$_2$O) indicates that the origin of both N atoms in N$_2$O is the pool of ^{15}NO$_2^-$, suggesting that under oxygen depletion, NO$_2^-$ is the only source of N atoms for N$_2$O formation, which is consistent with the observations by Kraft et al. (2022). It is worth highlighting that oxygen depletion is required for NO accumulation and, consequently, for NO dismutation to take place. At higher oxygen concentrations, NO would not accumulate to the concentrations observed in the incubations presented here because it reacts with oxygen via autooxidation, producing NO$_2^-$ (Ford et al., 1993; Hickok et al., 2013).

During the incubations with a pool of ^{15}NO$_2^-$, *N. maritimus* and *N. piranensis* accumulated oxygen, NO, and ^{46}N$_2$O and produced ^{30}N$_2$. In the incubations of *N. piranensis* with a pool of ^{14}NO$_2^-$, the spiked ^{46}N$_2$O resulted in the accumulation of ^{30}N$_2$, with N$_2$O being the only source of ^{15}N atoms to form dinitrogen. The quick consumption of the spiked N$_2$O shows that *N. maritimus* and *N. piranensis* quickly turn over the N$_2$O pool to N$_2$ when exposed to oxygen depletion. This evidence supports the role of N$_2$O as an intermediate in the NO-dismutation pathway. To the best of our knowledge, this is the first time that direct N$_2$O reduction to dinitrogen by AOA has been shown in physiology experiments.

When exposed to anoxia, NO dismutation is advantageous for AOA because it constitutes an alternative pathway to sustain energy generation and provides alternative electron acceptors and oxygen that can sustain ammonia oxidation at nanomolar ranges (Kraft et al., 2022). While the NO-dismutation reaction is electron-neutral, the other N-conversion steps in the pathway require electrons. The reduction of NO$_2^-$ to NO requires one electron per molecule of NO produced, and the reduction of N$_2$O to N$_2$ requires two electrons per molecule of N$_2$ produced. While the electrons could be partly supplied by ammonia oxidation, the source of the remaining electrons has yet to be discovered. Potential electron donors are organic compounds naturally accumulated in the culture medium during aerobic cell growth (Bayer et al., 2019, 2022).

If AOA were capable of using alternative electron donors other than ammonia, N$_2$O could serve as the sole electron acceptor under anoxia. The rapid conversion of N$_2$O to N$_2$ in the two AOA isolates investigated here supports this possibility. Metabolic activity and growth with N$_2$O as the only electron acceptor are common in many different denitrifying and non-denitrifying microorganisms, with a NosZ N$_2$O reductase (Mania et al., 2016; Conthe et al., 2018; Lycus et al., 2018; Read-Daily et al., 2022). Given the incubation times in the present study, cell growth was not expected to be observed. During aerobic ammonia oxidation under oxic and optimal conditions, AOA grow at a relatively slow rate. Generation times of *N. maritimus* and *N. piranensis* are at a minimum of 19 and 27 h, respectively (Qin et al., 2017; Bayer et al., 2019). Growth rates under anoxic conditions are expected to drop. Therefore, to detect cell growth when AOA perform NO dismutation under oxygen depletion, future research should explore alternatives to cell counts, such as using activity proxies like the incorporation of specifically labeled substrates (Musat et al., 2012; Hatzenpichler et al., 2020).

Although nitrite reduction to NO is most likely performed by the NirK nitrite reductase (Bartossek et al., 2010; Kozlowski et al., 2016), the enzymes responsible for NO dismutation and the further reduction of N$_2$O by AOA remain to be identified. No genes encoding potential NO dismutases or N$_2$O reductases have been identified in the genomes of *N. maritimus*, *N. piranensis,* or other AOA species (Walker et al., 2010; Qin et al., 2020). All known nitrous oxide reductases belong to the NosZ family. However, the existence of N$_2$O reductases outside of this family has been proposed multiple times, as reduction of N$_2$O has been observed in pure microbial cultures that lack a NosZ enzyme (Arciero et al., 2002; Fernandes et al., 2010). Recently, the cytochrome P450 was suggested to be involved in the production of N$_2$O via NO reduction by the AOA *Nitrosocosmicus oleophilus* MY3, based on N$_2$O production measurements coinciding with higher expression of the cytochrome (Jung et al., 2019). These observations were made under oxic conditions and low pH (5.5), in contrast to the conditions used in the current study (oxygen depletion and media HEPES buffered at a pH of 7.6). In *Ca. M. oxyfera*, quinol-dependent NO reductases (qNORs) have been identified as putative NO dismutases encoded by the *nod* gene (Ettwig et al., 2010, 2012; Zhu et al., 2019), but AOA do not possess these genes. To date, the potential for NO dismutation followed by N$_2$O reduction to N$_2$ by AOA would therefore be overlooked in comparative genomic analyses.

In physiological studies, NO dismutation by AOA would also have been easily overlooked because AOA cultures were not exposed long enough to oxygen depletion, and nitrogen compounds were studied with lower-resolution methods. The lowest oxygen concentrations examined in previous physiological studies of AOA were approximately 1 µM in the headspace (0.1%) (Qin et al., 2015, 2017), and ammonia oxidation was no longer detectable with colorimetric assays. These oxygen concentrations greatly exceed the concentrations at which we observed NO dismutation and oxygen accumulation. At the oxygen concentrations of the present study, the ammonia oxidation rates are in the range of 40 nM/h and would only be detectable by using ^{15}N-tracers, as shown by Kraft et al. (2022). Furthermore, the rates of N$_2$ production via NO dismutation are also low and would not be detectable without the use of ^{15}N-tracers.

Variability in oxygen accumulation trends in marine AOA

In oxygen-depleted incubations in which oxygen accumulation was observed in all replicates, oxygen accumulation often decreased toward the end of the incubation, similar to previous observations

(Kraft et al., 2022; Hernández-Magaña et al., 2023). The quick oxygen respiration after oxygen pulses, despite oxygen not being accumulated, indicates respiratory activity of the AOA cells (Figure 4). Moreover, the reduction of N_2O and constant production of N_2 in these incubations continued despite the apparent lack of oxygen accumulation. In the specific case of *N. piranensis,* oxygen did not accumulate in some incubation bottles (Figures 4C,D). After cyanide addition, a rapid increase in oxygen concentration was observed (Figure 4D and Supplementary Figure S7A). These observations, taken together, suggest that the cultures most likely continued to produce oxygen via NO dismutation, but all of it was utilized immediately, leading to no accumulation at detectable concentrations. Therefore, the lack of oxygen accumulation does not imply a lack of activity or absence of oxygen production, but most likely a more efficient usage of the oxygen produced, which prevents accumulation from being detected.

These observations point toward a change in the efficiency of the coupling between oxygen production and its use: at the beginning of the incubation, oxygen is produced faster than it is used, and later the production and consumption processes become more tightly coupled, or in the case of *N. piranensis*, some culture batches may have a faster response to oxygen depletion, which leads to a tighter coupling between oxygen production and consumption. Tightly coupled oxygen production and consumption takes place in cultures of the methane oxidizer *Ca. M. oxyfera*: no oxygen accumulates during NO dismutation, as it is immediately utilized intracellularly for methane oxidation (Ettwig et al., 2010). In *Ca. M. oxyfera*, the detection of oxygen produced via NO dismutation was only possible after the inhibition of the oxygen-consuming methane mono-oxygenase complex (pMMO) by acetylene (Ettwig et al., 2010, 2012; Wu et al., 2011), which is comparable to our observation of oxygen accumulation after cyanide addition.

Whether AOA are capable of producing oxygen via the NO-dismutation pathway in the environment is still unknown and challenging to detect, as any trace of oxygen produced in the environment would be immediately used by the microbial community (Garcia-Robledo et al., 2017), and because the isotopic signature of ^{15}N-tracer methods to detect NO dismutation is indistinguishable from denitrification. Therefore, it is important to perform investigations in environmental settings to unveil the potential influence of AOA activity on the oxygen and nitrogen metabolism of natural communities in oxygen-depleted ecosystems.

Conclusion

We confirmed that in the NO-dismutation pathway performed by AOA under oxygen depletion, N_2O is indeed an intermediate and demonstrated that NO is dismutated to oxygen and nitrous oxide, which is then further reduced to dinitrogen. Through incubations with combinations of different N compounds with different isotopic signatures ($^{15}NO_2^-$ pool $+^{44}N_2O$ spike and $^{14}NO_2^-$ pool $+^{46}N_2O$ spike), we showed that N_2O is rapidly turned over by AOA and that AOA are capable of reducing N_2O to N_2 at high rates. The observations made here highlight the importance of a new pathway of N_2O turnover by AOA, whose potential in the environment needs to be further investigated. AOA have been shown to be abundant in environments with short or extended periods of anoxia, such as marine OMZs or anoxic basins. Experimental evidence of AOA activity at such sites is crucial to determining the extent to which this pathway should be included among the potential sources and sinks of N_2O in the environment.

Data availability statement

The original contributions presented in the study are included in the article/Supplementary material, further inquiries can be directed to the corresponding authors.

Author contributions

EH-M: Conceptualization, Data curation, Formal analysis, Investigation, Methodology, Visualization, Writing – original draft, Writing – review & editing. BK: Conceptualization, Funding acquisition, Investigation, Supervision, Writing – original draft, Writing – review & editing, Methodology.

Conflict of interest

The authors declare that the research was conducted in the absence of any commercial or financial relationships that could be construed as a potential conflict of interest.

Publisher's note

All claims expressed in this article are solely those of the authors and do not necessarily represent those of their affiliated organizations, or those of the publisher, the editors and the reviewers. Any product that may be evaluated in this article, or claim that may be made by its manufacturer, is not guaranteed or endorsed by the publisher.

Supplementary material

The Supplementary material for this article can be found online at: https://www.frontiersin.org/articles/10.3389/fmicb.2024.1410251/full#supplementary-material

References

Arciero, D. M., Pierce, B. S., Hendrich, M. P., and Hooper, A. B. (2002). Nitrosocyanin, a red Cupredoxin-like protein from *Nitrosomonas europaea. Biochemistry* 41, 1703–1709. doi: 10.1021/bi015908w

Babbin, A. R., Bianchi, D., Jayakumar, A., and Ward, B. B. (2015). Rapid nitrous oxide cycling in the Suboxic Ocean. *Science* 348, 1127–1129. doi: 10.1126/science. aaa8380

Bartossek, R., Nicol, G. W., Lanzen, A., Klenk, H.-P., and Schleper, C. (2010). Homologues of nitrite reductases in ammonia-oxidizing archaea: diversity and genomic context. *Environ. Microbiol.* 12, 1075–1088. doi: 10.1111/j.1462-2920.2010.02153.x

Bayer, B., Hansman, R. L., Bittner, M. J., Noriega-Ortega, B. E., Niggemann, J., Dittmar, T., et al. (2019). Ammonia-oxidizing archaea release a suite of organic compounds potentially fueling prokaryotic heterotrophy in the ocean. *Environ. Microbiol.* 21, 4062–4075. doi: 10.1111/1462-2920.14755

Bayer, B., McBean, K., Carlson, C. A., and Santoro, A. E. (2022). Carbon content, carbon fixation yield and dissolved organic carbon release from diverse marine nitrifiers. *Limnol. Oceanography* 68, 84–96. doi: 10.1002/lno.12252

Beman, J. M., Popp, B. N., and Francis, C. A. (2008). Molecular and biogeochemical evidence for ammonia oxidation by marine Crenarchaeota in the Gulf of California. *ISME J.* 2, 429–441. doi: 10.1038/ismej.2007.118

Bristow, L. A., Dalsgaard, T., Tiano, L., Mills, D. B., Bertagnolli, A. D., Wright, J. J., et al. (2016). Ammonium and nitrite oxidation at nanomolar oxygen concentrations in oxygen minimum zone waters. *Proc. Natl. Acad. Sci.* 113, 10601–10606. doi: 10.1073/pnas.1600359113

Codispoti, L. A. (2010). Interesting times for marine N_2O. *Science* 327, 1339–1340. doi: 10.1126/science.1184945

Conthe, M., Wittorf, L., Kuenen, J. G., Kleerebezem, R., van Loosdrecht, M. C. M., and Hallin, S. (2018). Life on N_2O: deciphering the ecophysiology of N_2O respiring bacterial communities in a continuous culture. *ISME J.* 12, 1142–1153. doi: 10.1038/s41396-018-0063-7

Dalsgaard, T., Thamdrup, B., Farías, L., and Revsbech, N. P. (2012). Anammox and denitrification in the oxygen minimum zone of the eastern South Pacific. *Limnol. Oceanogr.* 57, 1331–1346. doi: 10.4319/lo.2012.57.5.1331

Ettwig, K. F., Butler, M. K., Le Paslier, D., Pelletier, E., Mangenot, S., Kuypers, M. M. M., et al. (2010). Nitrite-driven anaerobic methane oxidation by oxygenic bacteria. *Nature* 464, 543–548. doi: 10.1038/nature08883

Ettwig, K. F., Speth, D. R., Reimann, J., Wu, M. L., Jetten, M. S. M., and Keltjens, J. T. (2012). Bacterial oxygen production in the dark. *Front. Microbiol.* 3:273. doi: 10.3389/fmicb.2012.00273

Fernandes, A. T., Damas, J. M., Todorovic, S., Huber, R., Baratto, M. C., Pogni, R., et al. (2010). The multicopper oxidase from the archaeon *Pyrobaculum aerophilum* shows nitrous oxide reductase activity. *FEBS J.* 277, 3176–3189. doi: 10.1111/j.1742-4658.2010.07725.x

Ford, P. C., Wink, D. A., and Stanbury, D. M. (1993). Autoxidation kinetics of aqueous nitric oxide. *FEBS Lett.* 326, 1–3. doi: 10.1016/0014-5793(93)81748-O

Francis, C. A., Roberts, K. J., Beman, J. M., Santoro, A. E., and Oakley, B. B. (2005). Ubiquity and diversity of ammonia-oxidizing archaea in water columns and sediments of the ocean. *Proc. Natl. Acad. Sci.* 102, 14683–14688. doi: 10.1073/pnas.0506625102

Garcia-Robledo, E., Padilla, C. C., Aldunate, M., Stewart, F. J., Ulloa, O., Paulmier, A., et al. (2017). Cryptic oxygen cycling in anoxic marine zones. *Proc. Natl. Acad. Sci.* 114, 8319–8324. doi: 10.1073/pnas.1619844114

Hatzenpichler, R., Krukenberg, V., Spietz, R. L., and Jay, Z. J. (2020). Next-generation physiology approaches to study microbiome function at single cell level. *Nat. Rev. Microbiol.* 18, 241–256. doi: 10.1038/s41579-020-0323-1

Hernández-Magaña, A. E., Canfield, D. E., and Kraft, B. (2023). Oxygen production via NO dismutation in different ammonia oxidisers. *BioRxiv. [Preprint].* doi: 10.1101/2023.06.07.544047

Hickok, J. R., Vasudevan, D., Jablonski, K., and Thomas, D. D. (2013). Oxygen dependence of nitric oxide-mediated signaling. *Redox Biol.* 1, 203–209. doi: 10.1016/j.redox.2012.11.002

Hink, L., Lycus, P., Gubry-Rangin, C., Frostegård, Å., Nicol, G. W., Prosser, J. I., et al. (2017). Kinetics of NH_3-oxidation, NO-turnover, N_2O-production and electron flow during oxygen depletion in model bacterial and archaeal ammonia oxidisers. *Environ. Microbiol.* 19, 4882–4896. doi: 10.1111/1462-2920.13914

Jones, C. M., Graf, D. R., Bru, D., Philippot, L., and Hallin, S. (2013). The unaccounted yet abundant nitrous oxide-reducing microbial community: a potential nitrous oxide sink. *ISME J.* 7, 417–426. doi: 10.1038/ismej.2012.125

Jung, M.-Y., Gwak, J.-H., Rohe, L., Giesemann, A., Kim, J.-G., Well, R., et al. (2019). Indications for enzymatic denitrification to N_2O at low pH in an ammonia-oxidizing archaeon. *ISME J.* 13, 2633–2638. doi: 10.1038/s41396-019-0460-6

Karner, M. B., DeLong, E. F., and Karl, D. M. (2001). Archaeal dominance in the mesopelagic zone of the Pacific Ocean. *Nature* 409, 507–510. doi: 10.1038/35054051

Könneke, M., Bernhard, A. E., de la Torre, J. R., Walker, C. B., Waterbury, J. B., and Stahl, D. A. (2005). Isolation of an autotrophic ammonia-oxidizing marine archaeon. *Nature* 437, 543–546. doi: 10.1038/nature03911

Kozlowski, J. A., Stieglmeier, M., Schleper, C., Klotz, M. G., and Stein, L. Y. (2016). Pathways and key intermediates required for obligate aerobic ammonia-dependent chemolithotrophy in bacteria and Thaumarchaeota. *ISME J.* 10, 1836–1845. doi: 10.1038/ismej.2016.2

Kraft, B., Jehmlich, N., Larsen, M., Bristow, L. A., Könneke, M., Thamdrup, B., et al. (2022). Oxygen and nitrogen production by an ammonia-oxidizing archaeon. *Science* 375, 97–100. doi: 10.1126/science.abe6733

Lam, P., Jensen, M. M., Lavik, G., McGinnis, D. F., Müller, B., Schubert, C. J., et al. (2007). Linking crenarchaeal and bacterial nitrification to anammox in the Black Sea. *Proc. Natl. Acad. Sci.* 104, 7104–7109. doi: 10.1073/pnas.0611081104

Lehner, P., Larndorfer, C., Garcia-Robledo, E., Larsen, M., Borisov, S. M., Revsbech, N.-P., et al. (2015). LUMOS - a sensitive and reliable Optode system for measuring dissolved oxygen in the Nanomolar range. *PLoS One* 10:e0128125. doi: 10.1371/journal.pone.0128125

Löscher, C. R., Kock, A., Könneke, M., LaRoche, J., Bange, H. W., and Schmitz, R. A. (2012). Production of oceanic nitrous oxide by ammonia-oxidizing archaea. *Biogeosciences* 9, 2419–2429. doi: 10.5194/bg-9-2419-2012

Lycus, P., Soriano-Laguna, M. J., Kjos, M., Richardson, D. J., Gates, A. J., Milligan, D. A., et al. (2018). A bet-hedging strategy for denitrifying bacteria curtails their release of N_2O. *Proc. Natl. Acad. Sci.* 115, 11820–11825. doi: 10.1073/pnas.1805000115

Mania, D., Heylen, K., van Spanning, R. J. M., and Frostegård, Å. (2016). Regulation of nitrogen metabolism in the nitrate-ammonifying soil bacterium bacillus vireti and evidence for its ability to grow using N_2O as electron acceptor. *Environ. Microbiol.* 18, 2937–2950. doi: 10.1111/1462-2920.13124

Martens-Habbena, W., Berube, P. M., Urakawa, H., de la Torre, J. R., and Stahl, D. A. (2009). Ammonia oxidation kinetics determine niche separation of nitrifying Archaea and Bacteria. *Nature* 461, 976–979. doi: 10.1038/nature08465

Musat, N., Foster, R., Vagner, T., Adam, B., and Kuypers, M. M. M. (2012). Detecting metabolic activities in single cells, with emphasis on nanoSIMS. *FEMS Microbiol. Rev.* 36, 486–511. doi: 10.1111/j.1574-6976.2011.00303.x

IPCC, (2014). *Climate change 2014: Synthesis report. Contribution of working groups I, II and III to the fifth assessment report of the intergovernmental panel on climate change.* Eds. R. K. Pachauri and L. A. Meyer (Geneva, Switzerland: IPCC) pp. 151.

Peng, X., Fuchsman, C. A., Jayakumar, A., Oleynik, S., Martens-Habbena, W., Devol, A. H., et al. (2015). Ammonia and nitrite oxidation in the eastern tropical North Pacific. *Glob. Biogeochem. Cycles* 29, 2034–2049. doi: 10.1002/2015GB005278

Prosser, J. I., Hink, L., Gubry-Rangin, C., and Nicol, G. W. (2020). Nitrous oxide production by ammonia oxidizers: physiological diversity, niche differentiation and potential mitigation strategies. *Glob. Chang. Biol.* 26, 103–118. doi: 10.1111/gcb.14877

Qin, W., Carlson, L. T., Armbrust, E. V., Devol, A. H., Moffett, J. W., Stahl, D. A., et al. (2015). Confounding effects of oxygen and temperature on the TEX86 signature of marine Thaumarchaeota. *Proc. Natl. Acad. Sci.* 112, 10979–10984. doi: 10.1073/pnas.1501568112

Qin, W., Meinhardt, K. A., Moffett, J. W., Devol, A. H., Armbrust, E. V., Ingalls, A. E., et al. (2017). Influence of oxygen availability on the activities of ammonia-oxidizing archaea. *Environ. Microbiol. Rep.* 9, 250–256. doi: 10.1111/1758-2229.12525

Qin, W., Zheng, Y., Zhao, F., Wang, Y., Urakawa, H., Martens-Habbena, W., et al. (2020). Alternative strategies of nutrient acquisition and energy conservation map to the biogeography of marine ammonia-oxidizing archaea. *ISME J.* 14, 2595–2609. doi: 10.1038/s41396-020-0710-7

Read-Daily, B., Ben Maamar, S., Sabba, F., Green, S., and Nerenberg, R. (2022). Effect of nitrous oxide (N_2O) on the structure and function of nitrogen-oxide reducing microbial communities. *Chemosphere* 307:135819. doi: 10.1016/j.chemosphere.2022.135819

Santoro, A. E., Buchwald, C., McIlvin, M. R., and Casciotti, K. L. (2011). Isotopic signature of N2O produced by marine Ammonia-oxidizing Archaea. *Science* 333, 1282–1285. doi: 10.1126/science.1208239

Sollai, M., Villanueva, L., Hopmans, E. C., Reichart, G.-J., and Sinninghe Damsté, J. S. (2019). A combined lipidomic and 16S rRNA gene amplicon sequencing approach reveals archaeal sources of intact polar lipids in the stratified Black Sea water column. *Geobiology* 17, 91–109. doi: 10.1111/gbi.12316

Stein, L. Y., Klotz, M. G., Lancaster, K. M., Nicol, G. W., Qin, W., Schleper, C., et al. (2021). Comment on "a critical review on nitrous oxide production by Ammonia-oxidizing Archaea" by Lan Wu, Xueming Chen, Wei Wei, Yiwen Liu, Dongbo Wang, and Bing-Jie Ni. *Environ. Sci. Technol.* 55, 797–798. doi: 10.1021/acs.est.0c06792

Stieglmeier, M., Mooshammer, M., Kitzler, B., Wanek, W., Zechmeister-Boltenstern, S., Richter, A., et al. (2014). Aerobic nitrous oxide production through N-nitrosating hybrid formation in ammonia-oxidizing archaea. *ISME J.* 8, 1135–1146. doi: 10.1038/ismej.2013.220

Thomson, A. J., Giannopoulos, G., Pretty, J., Baggs, E. M., and Richardson, D. J. (2012). Biological sources and sinks of nitrous oxide and strategies to mitigate emissions. *Philos. Trans. R. Soc. Lond. Ser. B Biol. Sci.* 367, 1157–1168. doi: 10.1098/rstb.2011.0415

Tiano, L., Garcia-Robledo, E., and Revsbech, N. P. (2014). A new highly sensitive method to assess respiration rates and kinetics of natural planktonic communities by use of the switchable trace oxygen sensor and reduced oxygen concentrations. *PLoS One* 9:e105399. doi: 10.1371/journal.pone.0105399

Walker, C. B., de la Torre, J. R., Klotz, M. G., Urakawa, H., Pinel, N., Arp, D. J., et al. (2010). Nitrosopumilus maritimus genome reveals unique mechanisms for nitrification and autotrophy in globally distributed marine crenarchaea. *Proc. Natl. Acad. Sci.* 107, 8818–8823. doi: 10.1073/pnas.0913533107

Wan, X. S., Hou, L., Kao, S.-J., Zhang, Y., Sheng, H.-X., Shen, H., et al. (2023). Pathways of N$_2$O production by marine ammonia-oxidizing archaea determined from dual-isotope labeling. *Proc. Natl. Acad. Sci.* 120:e2220697120. doi: 10.1073/pnas.2220697120

Wilson, M. T., Antonini, G., Malatesta, F., Sarti, P., and Brunori, M. (1994). Probing the oxygen binding site of cytochrome c oxidase by cyanide. *J. Biol. Chem.* 269, 24114–24119. doi: 10.1016/S0021-9258(19)51055-9

Wu, L., Chen, X., Wei, W., Liu, Y., Wang, D., and Ni, B.-J. (2020). A critical review on nitrous oxide production by Ammonia-oxidizing Archaea. *Environ. Sci. Technol.* 54, 9175–9190. doi: 10.1021/acs.est.0c03948

Wu, M. L., Ettwig, K. F., Jetten, M. S. M., Strous, M., Keltjens, J. T., and Van Niftrik, L. (2011). A new intra-aerobic metabolism in the nitrite-dependent anaerobic methane-oxidizing bacterium Candidatus '*Methylomirabilis oxyfera*'. *Biochem. Soc. Trans.* 39, 243–248. doi: 10.1042/BST0390243

Zhu, B., Wang, J., Bradford, L. M., Ettwig, K., Hu, B., and Lueders, T. (2019). Nitric oxide dismutase (nod) genes as a functional marker for the diversity and phylogeny of methane-driven oxygenic Denitrifiers. *Front. Microbiol.* 10:1577. doi: 10.3389/fmicb.2019.01577